Charge-transfer effect on the linewidth of Fe $K\alpha$ x-ray fluorescence spectra

Jun Kawai, Chikashi Suzuki, and Hirohiko Adachi
Department of Metallurgy, Kyoto University, Sakyo-ku, Kyoto 606, Japan

Tokuzo Konishi
Asahi Chemical Industry Co. Ltd., Analytical Research Center, Samejima, Fuji 416, Japan

Yohichi Gohshi
Department of Industrial Chemistry, University of Tokyo, Hongo, Bunkyo-ku, Tokyo 113, Japan
(Received 3 February 1994)

High-resolution $K\alpha$ x-ray fluorescence spectra of FeO, Fe_2O_3, Fe_3O_4, $K_3[Fe(CN)_6]\cdot 3H_2O$, $K_4[Fe(CN)_6]$, and Fe (metal) are measured. It is found that the linewidth of Fe $K\alpha_1$ (K-L_3) does not follow Van Vleck's theorem for oxides, but it follows Van Vleck's theorem for cyanides; the line shapes of FeO, Fe_2O_3, and Fe_3O_4 are nearly identical. These results are rationalized by the spin-unrestricted DV-$X\alpha$ molecular-orbital calculations of model clusters. The model clusters we tried are $[FeO_6]^{10-}$, $[FeO_6]^{9-}$, $[Fe(CN)_6]^{3-}$, and $[Fe(CN)_6]^{4-}$ as model clusters of FeO, Fe_2O_3, $K_3[Fe(CN)_6]\cdot 3H_2O$, and $K_4[Fe(CN)_6]$, respectively. The electronic structures of these clusters are calculated for their ground states and $1s^{-1}$ hole states. It is concluded from these calculations that the charge-transfer effect induced by the creation of the $1s^{-1}$ core hole, which is the initial state of the $K\alpha$ x-ray emission, reduces the effective number of $3d$ unpaired electrons of iron oxides, resulting in the $K\alpha_1$ width being reduced from that expected from Van Vleck's theorem. On the other hand, the effective number of $3d$ unpaired electrons of cyanides in the ground state is conserved in the $1s^{-1}$ core-hole state. Thus Van Vleck's theorem holds for cyanides.

I. INTRODUCTION

X-ray spectra emitted by primary x-ray excitation are called x-ray fluorescence spectra. X-ray fluorescence spectra of transition-metal compounds were believed to reflect the spin state of the compounds.[1] That is to say, it was believed that the $K\alpha_{1,2}$ (K-$L_{3,2}$) linewidths were broader for higher-spin compounds and narrower for lower-spin compounds. In this context, it was proved that the linewidth was roughly proportional to $J(2S+1)$, where J is the exchange interaction energy between the core hole and $3d$ valence hole(s), and S the total spin vector of the $3d$ shell.[2] This is Van Vleck's theorem.[3,4] A more detailed calculation using multiplet wave functions was performed by Nefedov.[5] Van Vleck's theorem, or multiplet theory, was also applied to the interpretation of $K\beta_{1,3}$ (K-$M_{3,2}$) line shapes. The $K\beta_{1,3}$ lines of transition metals are accompanied by a low-energy satellite, $K\beta'$. The origin of the transition-metal $K\beta'$ satellite was interpreted as the result of spin-spin exchange splitting. Thus, in this theory, the $K\beta_{1,3}$ and $K\beta'$ line intervals of transition-metal compounds were roughly estimated from $J(2S+1)$ and the intensity ratio of $K\beta'$ to $K\beta_{1,3}$ by the ratio of multiplicity of states, $S/(1+S)$.[6,7] Srivastava and co-workers,[8,9] however, proposed that plasmon loss was the origin of the $K\beta'$ satellite of transition-metal compounds, resulting in better agreement between theory and experiment than with Van Vleck's theorem. Though Urch and Webber[10] had proposed that the $K\beta'$ line of transition-metal compounds was due to a charge-transfer process occurring simultaneously with the $3p \rightarrow 1s$ transition, their proposal did not attract any attention until recently. The importance of the charge-transfer effect[11-23] rather than the multiplet-splitting effect[4,24-31] for the origin of the line splittings of transition-metal x-ray photoelectron spectra (XPS) has been recognized and x-ray fluorescence spectra have been reanalyzed from the viewpoint of the charge-transfer effect rather than the exchange interaction, for Cu $K\alpha$,[32-34] Ni $K\beta$,[35,36] Cu $L\alpha$,[37-40] and Fe $K\alpha$.[41] The present paper reports the importance of this charge-transfer effect in Fe $K\alpha$; it has been briefly reported in Ref. 42.

II. EXPERIMENT

The samples measured were potassium hexacyanoferrate (II), $K_4[Fe(CN)_6\cdot 3H_2O$ (in what follows, we abbreviate this to $K_4[Fe(CN)_6]$, because no direct chemical bonds form between H_2O and Fe); potassium hexacyanoferrate (III), $K_3[Fe(CN)_6]$; the iron oxides FeO, Fe_2O_3, and Fe_3O_4; and metallic iron. All the samples but for the metal were in powder form. These powder samples were pressed into briquettes.

The spectrometer used was a gearless double-crystal [Si(220)+Si(220)] x-ray fluorescence spectrometer, Technos XFRA-2000 with a W anode x-ray tube (40 kV, 50 mA).[43] The spectrometer temperature was stabilized at 300.0 K. The dwelling time for one channel was typically 10 or 20 sec and there were a total of 500 channels. The scanning range was from 6380 to 6415 eV with 0.07 eV steps. Details were similar to those reported in Ref. 43.

III. RESULTS AND DISCUSSION

The measured x-ray fluorescence spectra are shown in Figs. 1–4. These spectra have been normalized to the spectral area between 6380 and 6415 eV; backgrounds have not been subtracted. Figure 1 compares the Fe (metal) $K\alpha_{1,2}$ spectrum with FeO $K\alpha_{1,2}$; these two spectra are significantly different. Figures 2 and 3 compare Fe_2O_3 and FeO, and Fe_3O_4 and FeO, respectively. It is easily seen from Figs. 2 and 3 that the spectra of FeO, Fe_2O_3, and Fe_3O_4 are almost identical. Figure 4 compares $K_3[Fe(CN)_6]$, $K_4[Fe(CN)_6]$, and FeO; these spectra are significantly different from each other; in fact, their peak positions, linewidths, and asymmetry indices are all different. It is found from Fig. 4 that the peak-shift ordering of $K\alpha_1$ is $K_4[Fe(CN)_6] < K_3[Fe(CN)_6] <$ FeO, which is different from that of $K\alpha_2$ ($K_3[Fe(CN)_6] < K_4[Fe(CN)_6] <$ FeO). The line shape compared with $K\alpha_1$ of $K\alpha_2$ is somewhat complicated because $K\alpha_2$ has extra linewidth due to the L_2L_3M Coster-Kronig lifetime effect. Thus, in the present paper, we concentrate our attention on the $K\alpha_1$ line shape. Since we believe that the most convenient index of the line shape is the full width at half maximum (FWHM), the measured $K\alpha_1$ FWHM's are tabulated in Table I together with FWHM's reported in the literature. Though in this table the data of Meisel and Nefedov[44] were measured with the highest resolution, they are only for high-spin compounds and the metal. On the other hand, the data of Leonhardt and Meisel[45] were restricted to the low-spin compounds, and the data for the common material (the metal) between Refs. 44 and 45 indicate that these two sets of data were measured with different spectrometer resolution. An iron compound becomes a high-spin state if the ligand-field splitting between t_{2g} and e_g is small because of a weak ligand (or crystal) field. This is the case of oxides. On the other hand, an iron compounds becomes a low-spin state if the ligand-field splitting is large because of a strong crystal field, or strong hybridization between the ligands and the center metal such as $K_3[Fe(CN)_6]$ or $K_4[Fe(CN)_6]$ (see Fig. 11 below). Though the data of Kashiwakura, Sukuzi, and Gohshi[46] indicate that the $K\alpha_1$ FWHM is proportional to the spin state, data for a divalent high-spin compound have not been reported. The data reported in the literature are not complete in themselves, because none of the papers reported all types of chemical states of iron compounds; 3+ and 2+ oxidation states, and high- and low-spin states. The present work reports all the chemical states of iron including the metal. The present result indicates that the $K\alpha_1$ FWHM of high-spin Fe^{3+} is not significantly broader than that of high-spin Fe^{2+}. We believe that the present data are reliable because the present FWHM's are quite close to those of Kashiwakura, Suzuki, and Gohshi,[46] in spite of the fact that they used a different double-crystal spectrometer (Toshiba AFV-701).

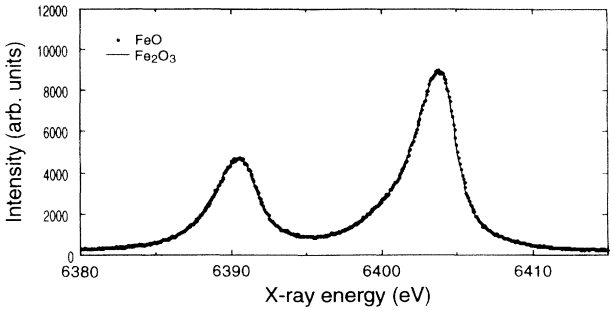

FIG. 2. Measured Fe $K\alpha_{1,2}$ x-ray fluorescence spectra of Fe_2O_3 and FeO.

To see more clearly the difference of the measured $K\alpha_1$ widths from those expected from Van Vleck's theorem, the measured FWHM's are plotted against the nominal number of unpaired $3d$ electrons in the compounds (Fig. 5). Van Vleck's theorem suggests the existence of rough proportionality between the number of unpaired $3d$ electrons and the FWHM, as indicated by the broken line in Fig. 5. This holds for $K_4[Fe(CN)_6]$ and $K_3[Fe(CN)_6]$; however, the linewidths of FeO, Fe_2O_3, and Fe_3O_4 seem to be narrower than those expected from Van Vleck's theorem, though Van Vleck's theorem is quite a rough rule. The measured FWHM saturates when the spin state becomes high spin. We rationalize this saturation in what follows using a molecular-orbital method including core-hole relaxation.

To clarify this saturation, we have calculated the electronic structure of both the ground state and the $1s^{-1}$ hole state of model clusters using the spin-unrestricted DV-$X\alpha$ molecular-orbital method.[47] Similar calculations were already reported by Sano, Adachi, and Yamatera[48] for $[Fe(CN)_6]^{3,4-}$ clusters. The model clusters used were

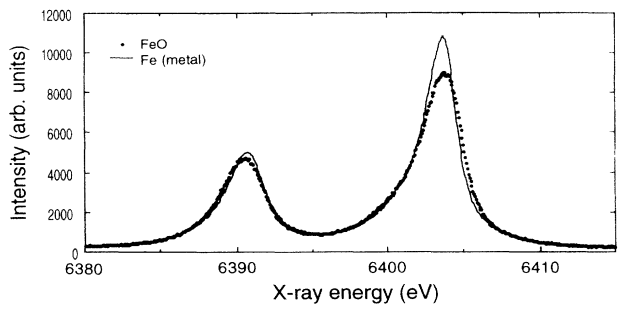

FIG. 1. Measured Fe $K\alpha_{1,2}$ x-ray fluorescence spectra of Fe (metal) and FeO.

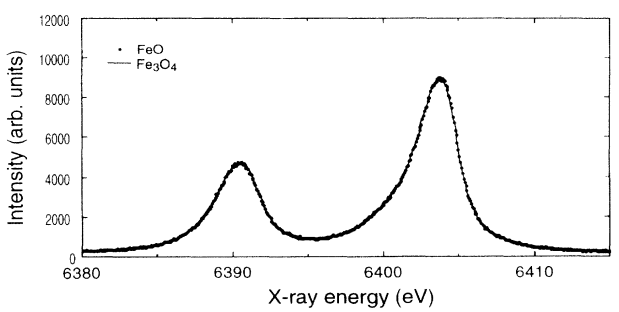

FIG. 3. Measured Fe $K\alpha_{1,2}$ x-ray fluorescence spectra of Fe_3O_4 and FeO.

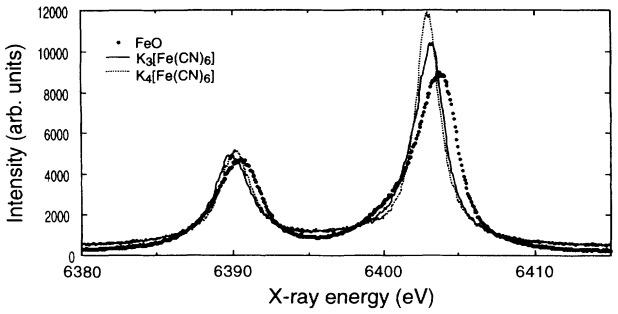

FIG. 4. Measured Fe $K\alpha_{1,2}$ x-ray fluorescence spectra of $K_3[Fe(CN)]_6$, $K_4[Fe(CN)]_6$, and FeO.

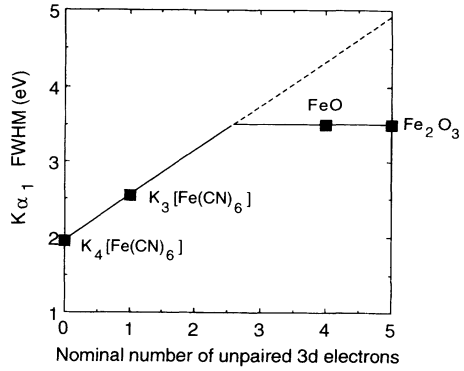

FIG. 5. Measured Fe $K\alpha_1$ FWHM plotted against the nominal number of unpaired $3d$ electrons in the ground state.

$[Fe(CN)_6]^{3,4-}$ and $[FeO_6]^{9,10-}$ as shown in Table II. Basis sets used were Fe $1s$-$4p$ and C, N, and O $1s$-$2p$. The clusters have O_h symmetry, and the geometry of these model clusters is shown in Table II. The atomic distances of these model clusters were taken to be the same for FeO and Fe_2O_3, and for $K_3[Fe(CN)_6]$ and $K_4[Fe(CN)_6]$. This was because only the effect of the change of the unpaired $3d$ electrons was required. The Fe-O distance of the model cluster FeO_6 was 2.10 Å; this was because the Fe-O distance is 1.945 or 2.116 Å in α-Fe_2O_3, and 2.15 Å in FeO.[49] To check the validity of taking Fe-O=2.10 Å, we calculated the electronic structure of $[FeO_6]^{10-}$ for various Fe-O distances as shown in Fig. 6. When Fe-O $\leq$ 1.7 Å, then the FeO became a low-spin compound[50,51] because of strong hybridization between Fe $3d$ and O $2p$ orbitals (strong crystal field). When Fe-O > 1.7 Å, the compound was a high-spin compound[50,51] because of the weak crystal field. Therefore the calculation was valid if the Fe-O distance was larger than 1.7 Å (critical length). The distance Fe-O=2.10 Å in the present calculation was larger than the critical length. The Fe-C and C-N distances of the model cluster $Fe(CN)_6$ were 1.90 and 1.15 Å, respectively. This was because C-N=1.15 Å in the HCN molecule,[52] and Fe-C=1.900 Å in $Cs_2Mg[Fe(CN)_6]$ and 1.926 Å in $Cs_2Li[Fe(CN)_6]$.[52]

The number of random sampling points in the DV-$X\alpha$ calculations was 2100 and 3900 for FeO_6 and $Fe(CN)_6$ clusters, respectively; 300 points per atom. Slater's exchange parameter (α) was fixed at 0.7 for all the atoms in the clusters. All the atoms were situated in a well potential of radius 4.0 bohrs and depth -2.0 hartrees to converge the atomic basis sets for negatively charged clusters.

The calculated Fe $3d$ and C and N $2p$ or O $2p$ densities of states (DOS's) in the ground state and $1s\uparrow^{-1}$ hole state are shown in Figs. 7–10. We have omitted showing the DOS's of the $1s\downarrow^{-1}$ hole states though we have calculated them, because they are almost identical to those of the $1s\uparrow^{-1}$ hole states. The plotted DOS's have been reduced to Fe-C-N or Fe-O (equivalent atomic percent) in place of $Fe(CN)_6$ and FeO_6; ligand DOS's were reduced to one-sixth to compare the DOS between Fe and ligand on the same scale. The gross atomic-orbital populations[53] of the Fe $3d$ and C, N, and O $2p$ orbitals are plotted against the molecular-orbital $X\alpha$ energy in Figs. 7–10, where the level width is broadened by a Gaussian function (0.2 eV FWHM) to mimic the solid state.

It is found from Figs. 7 and 8 that the energy separation between Fe $3d$ (indicated by e_g and t_{2g} in Figs. 7 and 8) and ligand $2p$ becomes smaller by 1.2 (t_{2g})–1.8 (e_g) eV; the level ordering essentially does not change for $[Fe(CN)_6]^{3,4-}$. That is to say, the $3d$ orbital is always shallower than the ligand $2p$ orbitals for both ground state and $1s^{-1}$ hole state. The levels become deeper by 6.2 eV (t_{2g}) and 5.0 eV (C and N $2p$) for both $[Fe(CN)_6]^{4-}$ and $[Fe(CN)_6]^{3-}$ clusters.

On the other hand, the levels become deeper by 11–12 eV for FeO, as easily calculated from Fig. 9. Comparing

TABLE I. Measured Fe $K\alpha_1$ FWHM (eV) in the literature and in the present work. (Definitions of low- and high-spin compounds, formal oxidation number, and the number of unpaired $3d$ electrons are also tabulated).

Spin state	Formal oxidation	Number of unpaired electrons	Compound	FWHM (eV) Ref. 44	Ref. 45	Ref. 46	Present work
Metal	0		Fe (metal)	2.41	3.16		2.69
Low spin	2+	0	$K_4[Fe(CN)_6]$		2.62	1.94	1.95
Low spin	3+	1	$K_3[Fe(CN)_6]$		2.99	2.59	2.54
High spin	2+	4	FeO	2.97			3.51
High spin	3+	5	Fe_2O_3	3.20		3.50	3.53

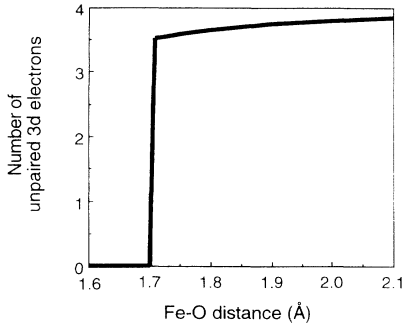

FIG. 6. Calculated number of unpaired $3d$ electrons with the change of Fe-O distance for $[FeO_6]^{10-}$ cluster.

Fig. 9(a) with 9(b), the Fe $3d\downarrow$ component mixes with the O $2p\downarrow$ orbital in the $3e_g\downarrow$ and $1t_{2g}\downarrow$ molecular orbitals. The most striking feature of the FeO DOS is that the Fe $3d\uparrow$ orbitals approximately equal $2t_{2g}\uparrow$ and $4e_g\uparrow$ molecular orbitals in the ground state, but they become $3e_g\uparrow$ and $1t_{2g}\uparrow$ orbitals in the $1s^{-1}$ hole state. Therefore the oxygen $2p\uparrow$ and Fe $3d\uparrow$ orbitals cross each other on going from the ground state to the $1s^{-1}$ core-hole state.

The levels become deeper by ca. 8 eV for all the valence levels of Fe_2O_3. The Fe $3d\downarrow$ component also mixes with O $2p\downarrow$ in the $1t_{2g}\downarrow$ and $3e_g\downarrow$ molecular orbitals. The Fe $3d\uparrow$ orbitals of Fe_2O_3 equal $1t_{2g}\uparrow$ and $3e_g\uparrow$ both in the ground state and in the $1s^{-1}$ hole state. A very interesting feature is that the DOS of the Fe_2O_3 ground state [Fig. 10(a)] is quite similar to that of the FeO $1s^{-1}$ hole state [Fig. 9(b)]. The deepening of Fe_2O_3 (8 eV) is smaller than that of FeO (11–12 eV), which indicates that the valence molecular orbitals of Fe_2O_3 hybridize more strongly than those of FeO, or, in other words, electron correlation in Fe_2O_3 is stronger than in FeO. Torrance *et al.*[54] listed the $3d$ correlation energy[55,56] as α-Fe_2O_3 > FeO. Our present calculation supports this tendency. The level deepening of $Fe(CN)_6$ clusters is half that of FeO_6 clusters. This is because the $3d$ electrons are much more delocalized in $Fe(CN)_6$ clusters than in FeO_6 clusters. It is concluded from the level deepening that the d-electron delocalization ordering is $[Fe(CN)_6]^{3-}$ $=[Fe(CN)_6]^{4-}$ $>[FeO_6]^{9-}(Fe_2O_3)$ $>[FeO_6]^{10-}(FeO)$. Thus the $1s^{-1}$ core hole is well screened by the $3d$ electrons in the $Fe(CN)_6$ cluster, while the $1s^{-1}$ core hole is poorly screened by the $3d$ electrons in FeO_6 clusters. The $1s^{-1}$ core holes in the FeO_6 clusters are thus screened by the ligand $2p$ electrons. This is the reason for the charge transfer from the ligand to the $3d$ unoccupied levels.

In the case of Fe_3O_4, $Fe^{3+}(Fe^{2+}Fe^{3+})O_4$, where one-third of the Fe^{3+} ions occupy tetrahedral interstices, equal numbers of Fe^{2+} and Fe^{3+} ions occupy ocatahedral interstices; though we have not calculated the four-coordinated iron oxide clusters, the ligand-field splittings are complementary to those of six-coordinated iron oxides. Thus $e^3t_2^3$ for Fe^{2+} and $e^2t_2^3$ for Fe^{3+} are probably similar to the six-coordinated iron oxides with respect to the response to core-hole creation.

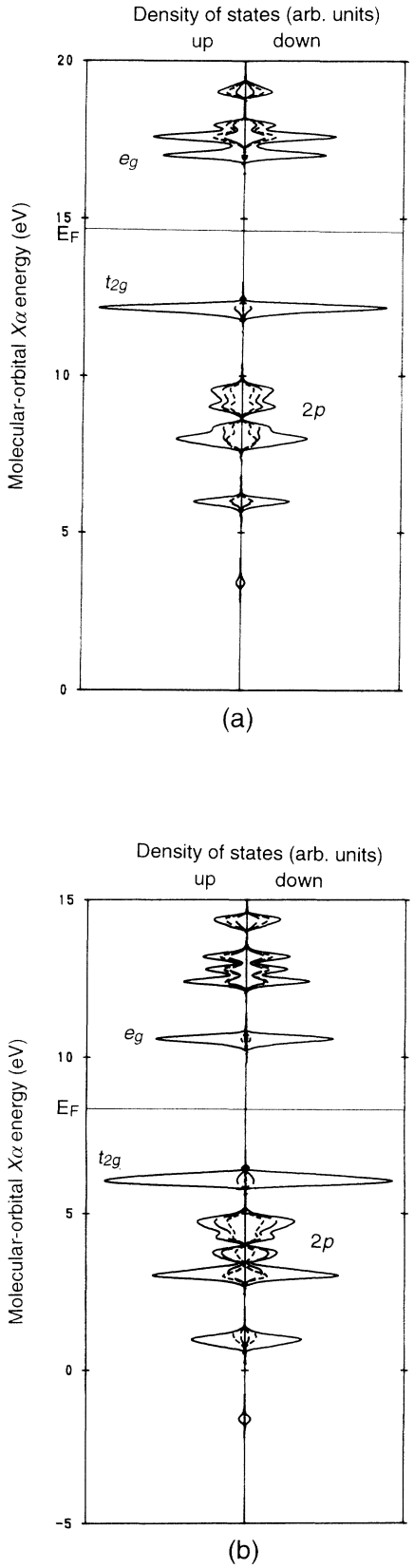

FIG. 7. Calculated Fe $3d$ and C and N $2p$ DOS's of $[Fe(CN)_6]^{4-}$ cluster in the ground state (a) and $1s\uparrow^{-1}$ core-hole state (b). Dotted line: C $2p$, broken line: N $2p$, full line: Fe $3d$ + C $2p$ + N $2p$. (Model of $K_4[Fe(CN)_6]$.)

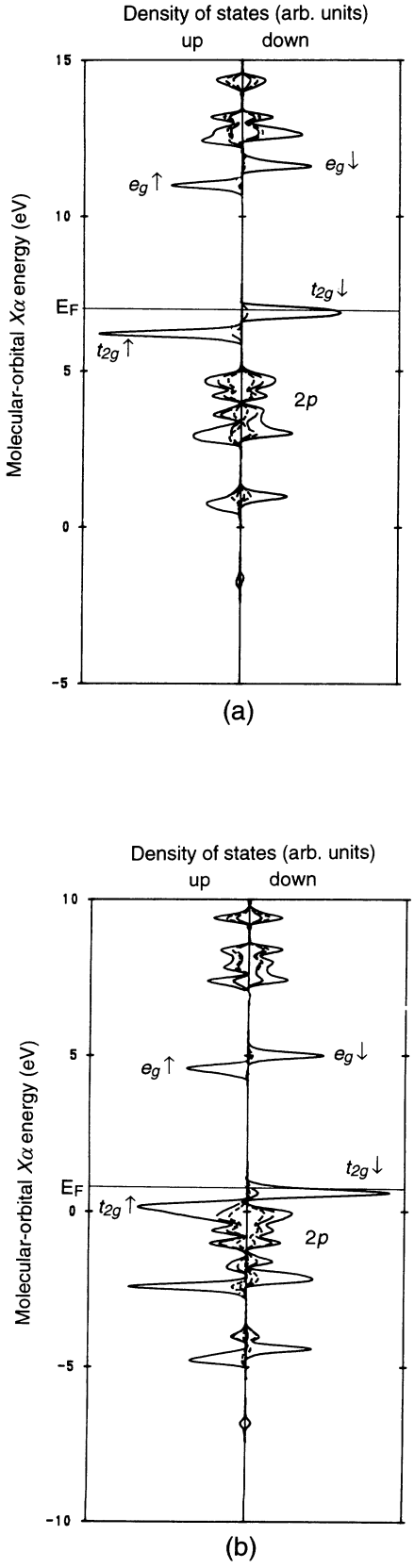

FIG. 8. Calculated Fe $3d$ and C and N $2p$ DOS's of $[Fe(CN)_6]^{3-}$ cluster in the ground state (a) and $1s\uparrow^{-1}$ core-hole state (b). Dotted line: C $2p$, broken line: N $2p$, full line: Fe $3d+C\,2p+N\,2p$. (Model of $K_3Fe(CN)_6$].)

To see more clearly the core-hole creation effect, we have calculated the gross atomic-orbital population[53] of Fe $3d$, $4s$, and $4p$ orbitals as shown in Tables III–VI. The negative values in Table III originate from the definition of the gross atomic-orbital population by Mulliken. Since $4s$ and $4p$ orbital components are minor, and since they delocalize in the clusters, we have omitted

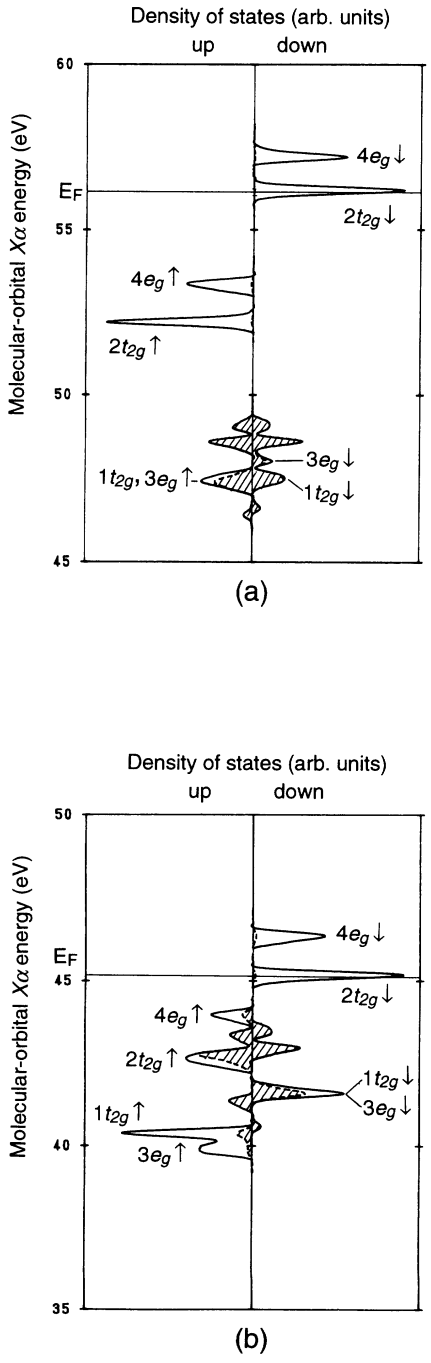

FIG. 9. Calculated Fe $3d$ and O $2p$ DOS's of $[FeO_6]^{10-}$ cluster in the ground state (a) and $1s\uparrow^{-1}$ core-hole state (b). Dotted line (hatched): O $2p$, full line: Fe $3d+O\,2p$. (Model of FeO.)

TABLE II. Calculated effective number of unpaired $3d$ electrons using the DV-$X\alpha$ molecular-orbital method.

Compounds	$K_4[Fe(CN)_6]$	$K_3[Fe(CN)_6]$	FeO	Fe_2O_3
Model cluster	$[Fe(CN)_6]^{4-}$	$[Fe(CN)_6]^{3-}$	$[FeO_6]^{10-}$	$[FeO_6]^{9-}$
Cluster geometry (O_h symmetry)	Fe-C=1.93 Å C-N=1.15 Å	Fe-C=1.93 Å C-N=1.15 Å	Fe-O=2.10 Å	Fe-O=2.10 Å
Nominal unpaired $3d$ electrons	0	1	4	5
Calculated effective unpaired electrons (ground state)	0.0	0.9	3.8	4.4
Calculated effective unpaired electrons ($1s^{-1}$ hole state)	0.0	0.7	3.2	3.3

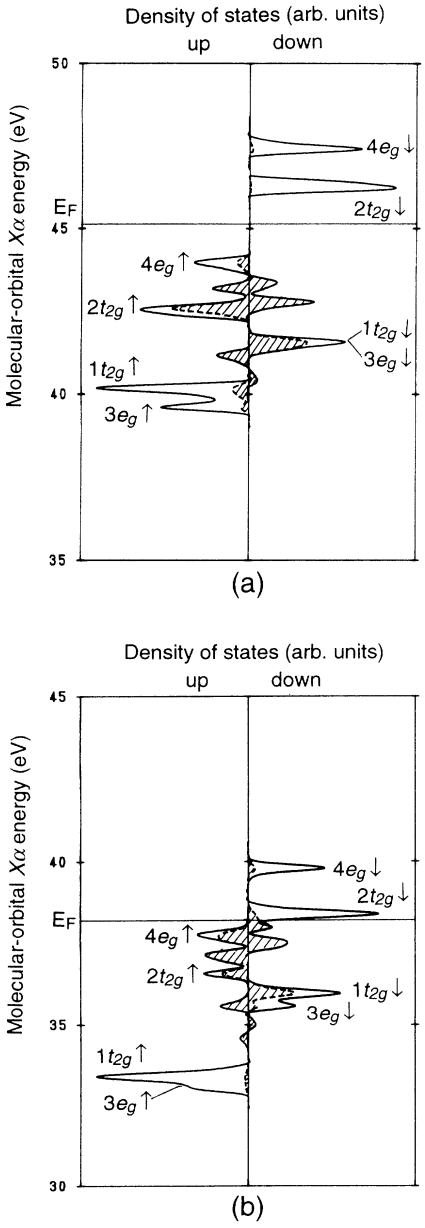

FIG. 10. Calculated Fe $3d$ and O $2p$ DOS's of $[FeO_6]^{9-}$ cluster in the ground state (a) and $1s\uparrow^{-1}$ core-hole state (b). Dotted line (hatched): O $2p$, full line: Fe $3d$+O $2p$. (Model of Fe_2O_3.)

them and only the differences $3d\uparrow$-$3d\downarrow$ are listed in Table II. The calculated effective numbers of $3d$ unpaired electrons ($3d\uparrow$-$3d\downarrow$) are 0.0, 0.9, 3.8, and 4.4 for $[Fe(CN)_6]^{4-}$, $[Fe(CN)_6]^{3-}$, $[FeO_6]^{10-}$, and $[FeO_6]^{9-}$, respectively, as shown in Table II. This means that the nominal one $3d$ electron equals effectively 0.88–0.95 electrons within the framework of the Mulliken population analysis. The most striking feature of the population analysis is that, while the effective $3d$ unpaired electron numbers of the $[Fe(CN)_6]^{3,4-}$ core-hole state conserve the values of the ground state, the number decreases in the core-hole state of $[FeO_6]^{10-}$ and $[FeO_6]^{9-}$ by 0.6 and 1.1 respectively, from the ground state. This indicates that one (two) electron(s) is (are) transferred from oxygen to the Fe $3d\downarrow$ orbital for FeO (Fe_2O_3). These charge-transfer effects are schematically shown in Fig. 11. They are similar to the effects seen in the core-hole state of copper oxides by XPS.[20] This type of charge transfer is possible for charge-transfer compounds (late transition-metal compounds), as classified by Zaanen, Sawatky, and Allen;[55] however the charge transfer is not possible for compounds with a well delocalized (or strongly correlated) d-electron system, such as $[Fe(CN)_6]^{3,4-}$.

Reference 1 reports that the linewidths of low-spin Fe^{3+}, high-spin Fe^{2+}, and high-spin Fe^{3+} are respectively 0.31, 1.37, and 1.42 eV broader than that of low-spin Fe^{2+}; the linewidth of Fe_2O_3 is 0.04 eV broader than that of FeO. In the present measurements, the linewidth of Fe_2O_3 is significantly (0.02 eV) broader than that of FeO as shown in Table I. Since we use the self-consistent field

TABLE III. Calculated effective number of valence electrons of the $[Fe(CN)_6]^{4-}$ cluster.

	Ground state	$1s\uparrow^{-1}$ hole state	$1s\downarrow^{-1}$ hole state
$3d\uparrow$	3.28	3.70	3.70
$3d\downarrow$	3.28	3.70	3.70
$4s\uparrow$	0.01	0.04	0.05
$4s\downarrow$	0.01	0.05	0.04
$4p\uparrow$	0.19	0.25	0.26
$4p\downarrow$	0.19	0.26	0.25
Sum	6.96	8.00	8.00

TABLE IV. Calculated effective number of valence electrons of the $[Fe(CN)_6]^{3-}$ cluster.

	Ground state	$1s\uparrow^{-1}$ hole state	$1s\downarrow^{-1}$ hole state
$3d\uparrow$	3.64	3.95	3.95
$3d\downarrow$	2.70	3.27	3.27
$4s\uparrow$	0.06	0.04	0.10
$4s\downarrow$	0.04	0.09	0.08
$4p\uparrow$	0.24	0.25	0.26
$4p\downarrow$	0.19	0.22	0.21
Sum	6.87	7.82	7.87

TABLE VI. Calculated effective number of valence electrons of the $[FeO_6]^{9-}$ cluster.

	Ground state	$1s\uparrow^{-1}$ hole state	$1s\downarrow^{-1}$ hole state
$3d\uparrow$	5.00	5.00	5.00
$3d\downarrow$	0.62	1.67	1.67
$4s\uparrow$	0.07	0.10	0.11
$4s\downarrow$	0.02	0.07	0.07
$4p\uparrow$	0.04	0.10	0.10
$4p\downarrow$	0.01	0.08	0.08
Sum	5.76	7.02	7.03

(SCF) method to calculate the electronic structure of the core-hole state, the present calculation is the adiabatic limit of the valence-electron response due to the $1s^{-1}$ core hole. Therefore the calculated energy levels of Figs. 7(b)–10(b) are the adiabatic limit, or, in other words, the results at infinitely long time for the core photoionization process. However, in the real case, the $1s^{-1}$ core-hole lifetime is 10^{-15} sec and the orbital relaxation time is one or less orders of magnitude shorter than the lifetime.[57] Therefore the energy levels shown in Figs. 7(b)–10(b) are not the only ones of the core-hole states, but they mix with other nonrelaxed states in the sudden limit.[58] The real states are well described by the sudden approximation as follows:

$$|K_4[Fe(CN)_6]\ 1s^{-1}\rangle = |Fe\ 1s^1 3d^6\rangle ,$$

$$|K_3[Fe(CN)_6]\ 1s^{-1}\rangle = |Fe\ 1s^1 3d^5\rangle ,$$

$$|FeO\ 1s^{-1}\rangle = C_1|Fe\ 1s^1 3d^7\ O\ 2p^5\rangle + C_2|Fe\ 1s^1 3d^6\ O\ 2p^6\rangle ,$$

$$|Fe_2O_3\ 1s^{-1}\rangle = C_1|Fe\ 1s^1 3d^7\ O\ 2p^4\rangle + C_2|Fe\ 1s^1 3d^6\ O\ 2p^5\rangle + C_3|Fe\ 1s^1 3d^5\ O\ 2p^6\rangle .$$

TABLE V. Calculated effective number of valence electrons of the $[FeO_6]^{10-}$ cluster.

	Ground state	$1s\uparrow^{-1}$ hole state	$1s\downarrow^{-1}$ hole state
$3d\uparrow$	5.00	5.00	5.00
$3d\downarrow$	1.20	1.78	1.78
$4s\uparrow$	0.00	0.07	0.07
$4s\downarrow$	−0.03	0.04	0.03
$4p\uparrow$	−0.05	0.04	0.04
$4p\downarrow$	−0.03	0.02	0.02
Sum	6.09	6.95	6.94

The major term is the first term; C_1 is largest. However, the second and third terms are not negligibly small; they have a larger linewidth because of multiplet splittings. Therefore the linewidth of Fe_2O_3 is a little bit broader than that of FeO as is shown in Table I.

IV. CONCLUSIONS

X-ray fluorescence $K\alpha$ spectra of various iron compounds were measured and it was found that the linewidths of iron oxides were too narrow compared with the widths expected from multiplet splittings due to the exchange interaction. These anomalies in line shapes were rationalized by electronic-structure calculations of cluster molecules for the ground and $1s^{-1}$ core-hole states. The numbers of unpaired $3d$ electrons do not change from the ground state to the core-hole state for cyanoferrates; one or two electrons were transferred from the oxygen $2p$ to the iron $3d$ orbital due to the core-hole positive charge for iron oxides, which reduces the numbers of unpaired $3d$ electrons in the $1s^{-1}$ core-hole state

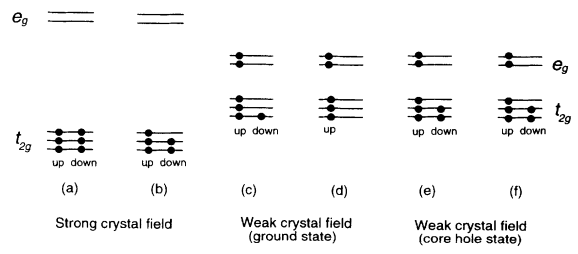

FIG. 11. Schematic energy-level diagrams and electron configurations of (a) $[Fe(CN)_6]^{4-}$ (ground state and $1s^{-1}$ core-hole state), (b) $[Fe(CN)_6]^{3-}$ (ground state and $1s^{-1}$ core-hole state), (c) $[FeO_6]^{10-}$ (ground state), (d) $[FeO_6]^{9-}$ (ground state), (e) $[Fe(CN)_6]^{10-}$ ($1s^{-1}$ core-hole state), and (f) $[FeO_6]^{9-}$ ($1s^{-1}$ core-hole state).

compared with those of the ground states. This is the reason why the iron oxide $K\alpha_1$ line shapes were too narrow compared with those expected from Van Vleck's theorem.

ACKNOWLEDGMENT

Thanks are due to Professor C. Satoko for fruitful discussions.

[1]J. Finster, G. Leonhardt, and A. Meisel, J. Phys. (Paris) Colloq. **32**, C4-218 (1971).

[2]K. Tsutsumi and H. Nakamori, in *Proceedings of the International Symposium on X-Ray Spectra and Electronic Stucture of Matter, München, 1972,* edited by A. Faessler and G. Wiech (Universität München, München, 1973), Vol. 1, p. 100.

[3]I. G. Batirev, J. A. Leiro, and M. Heinonen, in *Physics of Transition Metals,* edited by P. M. Oppeneer and J. Kübler (World Scientific, Singapore, 1993), Vol. II, pp. 926–929.

[4]S. P. Kowalczyk, L. Ley, R. A. Pollak, F. R. McFeely, and D. A. Shirley, Phys. Rev. B **7**, 4009 (1973).

[5]V. I. Nefedov. Izv. Akad. Nauk SSSR, Ser. Fiz. **28**, 816 (1964) [Bull. Acad. Sci. USSR, Phys. Ser. **28**, 724 (1964)].

[6]K. Tsutsumi, J. Phys. Soc. Jpn. **14**, 1696 (1959).

[7]K. Tsutsumi and H. Nakamori, J. Phys. Soc. Jpn. **25**, 1418 (1968).

[8]K. S. Srivastava, R. L. Shrivastava, O. K. Harsh, and V. Kumar, Phys. Rev. B **19**, 4336 (1979).

[9]K. S. Srivastava, S. Singh, A. K. Shrivastava, R. S. Nayal, A. Chaubey, and P. Gupta, Phys. Rev. A **25**, 2838 (1982).

[10]D. S. Urch and S. Webber, X-Ray Spectrom. **6**, 64 (1977).

[11]A. Kotani and Y. Toyozawa, J. Phys. Soc. Jpn. **37**, 563 (1974).

[12]A. Kotani and Y. Toyozawa, J. Phys. Soc. Jpn. **37**, 912 (1974).

[13]S. Larsson and M. Braga, Chem. Phys. Lett. **48**, 596 (1977).

[14]W. Domcke, L. S. Cederbaum, J. Schirmer, and W. von Niessen, Phys. Rev. Lett. **42**, 1237 (1979).

[15]J. C. Fuggle, M. Campagna, Z. Zolnierek, R. Lässer, and A. Platau, Phys. Rev. Lett. **45**, 1597 (1980).

[16]G. van der Laan, C. Westra, C. Haas, and G. A. Sawatzky, Phys. Rev. B **23**, 4369 (1981).

[17]B. W. Veal and A. P. Paulikas, Phys. Rev. B **31**, 5399 (1985).

[18]B. W. Veal, D. E. Ellis, and D. J. Lam, Phys. Rev. B **32**, 5391 (1985).

[19]A. Fujimori, M. Saeki, N. Kimizuka, M. Taniguchi, and S. Suga, Phys. Rev. B **34**, 7318 (1986).

[20]J. Ghijsen, L. H. Tjeng, J. van Elp, H. Eskes, J. Westerink, G. A. Sawatzky, and M. T. Czyzyk, Phys. Rev. B **38**, 11 322 (1988).

[21]G. Lee and S.-J. Oh, Phys. Rev. B **43**, 14 674 (1991).

[22]M. A. van Veenendaal and G. A. Sawatzky, Phys. Rev. Lett. **70**, 2459 (1993).

[23]G.-H. Gweon, J.-G. Park, and S.-J. Oh, Phys. Rev. B **48**, 7825 (1993).

[24]C. S. Fadley, D. A. Shirley, A. J. Freeman, P. S. Bagus, and J. V. Mallow, Phys. Rev. Lett. **23**, 1397 (1969).

[25]C. S. Fadley and D. A. Shirley, Phys. Rev. A **2**, 1109 (1970).

[26]D. C. Frost, C. A. McDowell, and I. S. Woolsey, Chem. Phys. Lett. **17**, 320 (1972).

[27]P. S. Bagus, A. J. Freeman, and F. Sasaki, Phys. Rev. Lett. **30**, 850 (1973).

[28]S. P. Kowalczyk, L. Ley, R. A. Pollak, F. R. McFeely, and D. A. Shirley, Phys. Rev. B **7**, 4009 (1973).

[29]R. P. Gupta and S. K. Sen, Phys. Rev. B **10**, 71 (1974).

[30]R. P. Gupta and S. K. Sen, Phys. Rev. B **12**, 15 (1975).

[31]T. Yamaguchi, S. Shibuya, and S. Sugano, J. Phys. C **15**, 2625 (1982).

[32]J. Kawai, Y. Nihei, M. Fujinami, Y. Higashi, S. Fukushima, and Y. Gohshi, Solid State Commun. **70**, 567 (1989).

[33]M. S. Osadchii and V. V. Murakhtanov, Zh. Strukt. Khim. **33** (4), 8 (1992) [J. Struct. Chem. **33**, 487 (1992)].

[34]M. S. Osadchii and V. V. Murakhtanov, É. S. Fomin, and L. N. Mazalov, Zh. Eksp. Teor. Fiz. **101**, 1259 (1992) [Sov. Phys. JETP **74**, 674 (1992)].

[35]J. Kawai, M. Takami, and C. Satoko, Phys. Rev. Lett. **65**, 2193 (1990).

[36]J. Kawai, Nucl. Instrum. Methods Phys. Res. Sect. B **75**, 3 (1993).

[37]J. Kawai and K. Maeda, Spectrochim. Acta Part B **46**, 1243 (1991).

[38]J. Kawai and K. Maeda, Physica C **185-189**, 981 (1991).

[39]J. Kawai, K. Nakajima, K. Maeda, and Y. Gohshi, Adv. X-ray Anal. **35**, 1107 (1992).

[40]J. Kawai, K. Maeda, K. Nakajima, and Y. Gohshi, Phys. Rev. B **48**, 8560 (1993).

[41]G. Dräger, W. Czolbe, and J. A. Leiro, Phys. Rev. B **45**, 8283 (1992).

[42]J. Kawai, Nucl. Instrum. Methods Phys. Res. Sect. B **87**, 88 (1994).

[43]T. Konishi, K. Nishihagi, and K. Taniguchi, Rev. Sci. Instrum. **62**, 2588 (1991).

[44]A. Meisel and W. Nefedow, Z. Phys. Chem. **219**, 194 (1962).

[45]G. Leonhardt and A. Meisel, Spectroschim. Acta Part B **25**, 163 (1970).

[46]J. Kashiwakura, I. Suzuki, and Y. Gohshi, Adv. X-Ray Chem. Anal. Jpn. **8**, 29 (1976).

[47]H. Adachi, S. Shiokawa, M. Tsukada, C. Satoko, and S. Sugano, J. Phys. Soc. Jpn. **47**, 1528 (1979).

[48]M. Sano, H. Adachi, and H. Yamatera, Bull. Chem. Soc. Jpn. **54**, 2898 (1981).

[49]A. F. Wells, *Structural Inorganic Chemistry,* 5th ed. (Oxford University Press, Oxford, 1984), pp. 545,551.

[50]S. Sugano, Y. Tanabe, and H. Kamimura, *Multiplets of Transition-Metal Ion in Crystals* (Academic, New York, 1970).

[51]B. N. Figgis, *Introduction to Ligand Fields* (Wiley, New York, 1966).

[52]*Kagaku Binran Kisohen II,* 4th ed., edited by Y. Morino (Maruzen, Tokyo, 1993), pp. II-653, II-664 (in Japanese).

[53]R. S. Mulliken, J. Chem. Phys. **23**, 1833 (1955).

[54]J. B. Torrance, P. Lacorro, C. Asavaroengchai, and R. M. Metzger, J. Solid State Chem. **90**, 168 (1991).

[55]J. Zaanen, G. A. Sawatzky, and J. W. Allen, Phys. Rev. Lett. **55**, 418 (1985).

[56]A. Fujimori, J. Phys. Chem. Solids **53**, 1595 (1992).

[57]D. J. Nagel, Adv. X-Ray Anal. **13**, 183 (1970); A. Meisel, G. Leonhardt, and R. Szargan, *X-Ray Spectra and Chemical Binding* (Springer, Berlin, 1989), p. 8.

[58]T. Åberg, Phys. Rev. **156**, 35 (1967).